

Spin inelastic currents in molecular ring junctions

Dhurba Rai* and Michael Galperin†

Department of Chemistry and Biochemistry, University of California at San Diego, La Jolla, CA 92093, USA

(Received 30 April 2012; revised manuscript received 11 June 2012; published 13 July 2012)

Within a simple model, we discuss spin inelastic currents in molecular ring junctions. We generalize considerations of the spin-flip inelastic electron tunneling spectroscopy (IETS) to the case of multisite molecular system, and formulate a conserving approximation, which takes into account renormalization of elastic channel. We also extend recent studies of circular currents in molecular junctions beyond scattering theory formulation. We demonstrate control of the spin-flip IETS signal and discuss spin polarization of total and circular currents in a benzene ring junction.

DOI: [10.1103/PhysRevB.86.045420](https://doi.org/10.1103/PhysRevB.86.045420)

PACS number(s): 85.65.+h, 85.35.Ds, 85.75.Mm, 71.70.Gm

I. INTRODUCTION

Advances in experimental techniques at nanoscale shift focus of research in molecular electronics^{1–5} from ballistic transport^{6–8} to inelastic effects^{9–11,13} (and closely related energy transfer processes^{12,14–18}), to noise characteristics,^{19–21} and optical response^{22–26} in current carrying junctions. Recent spin-transport experiments^{27,28} demonstrated potential possibility of using organic molecules to construct molecular spin devices, indicating the emergence of molecular spintronics^{30–35} (see Ref. 29 for a comprehensive review).

The small size of molecules implies potential importance of coherence in molecular junctions. Interference effects in molecular systems were observed experimentally for electron transfer³⁶ and molecular junction currents³⁷ involving derivatives of benzene connected in the meta or para positions. Effects of exciton coherence in photosynthesis were demonstrated in Ref. 38. Coherent control in molecular junctions was extensively discussed in theoretical literature.^{39–45} In particular, quantum interference plays a decisive role in conduction through molecular ring structures. Magnetic field control of electron conduction in such systems was considered in Refs. 46,47. The possibility to utilize interference effects in nanosized rings for constructing molecular spin filters was also discussed in the literature.^{48–51}

Another closely related issue in spintronics is the control of a local spin. In particular, spin control with electric currents achieved in experiments on single atoms⁵² and single-molecule magnets,⁵³ was studied theoretically in Refs. 54 and 55. On the other side, characteristics of local spin in junction conductance manifest themselves in spin-flip inelastic electron tunneling spectroscopy (IETS). Like in the usual IETS where electron coupling to molecular vibration results in appearance of steplike features in conductance on the scale of molecular vibrations (0.01–0.1 eV), energy exchange between tunneling electrons and the local spin system yields similar IETS signal in the micro-electron-volt range. Such spin-flip spectroscopy was demonstrated using STM on single atoms,⁵⁶ atomic structures,^{57,58} and molecular thin films.⁵⁹ Model based^{60–65} and *ab initio*⁶⁶ theoretical treatments are available in the literature for STM setup, where electron tunneling between tip and substrate interacts with a system of local spins via spin-spin exchange. A nonequilibrium Green function (NEGF) formulation for a model explicitly including system (single level) coupled to two electronic reservoirs (tip and substrate)

with treating spin-spin exchange interaction taken into account within the first Born approximation (BA) was presented in Ref. 67.

In this paper, we study spin inelastic current in a junction formed by a molecular ring (benzene) coupled to two metal leads. The spin-flip IETS signal is due to exchange interaction between conduction electrons and a local spin placed at the center of the ring. Thus the model combines consideration of quantum interference effects inherent in electron conduction in the molecular ring structures with spin-flip IETS due to interaction with local spin. We note that magnetic impurity placed at the ring center is an idealization, the only condition for the practical relevance of our model requires impurity in the vicinity of the benzene ring, which induces the spin-spin exchange interaction. Such structures have been studied both experimentally^{68,69} and theoretically.^{70–74}

We study inelastic effects in the (spin-resolved) total and circular currents within the NEGF approach. Circular currents are defined following the procedure outlined in Ref. 75. Since BA is a nonconserving approximation, a more advanced treatment is required for any system beyond single level (see, e.g., Ref. 77 for discussion). Here, we consider the spin-spin exchange interaction within the self-consistent BA (SCBA). The SCBA enforces conservation laws⁷⁶ and accounts for the renormalization of the elastic channel disregarded in Refs. 60–65, and 67. We also discuss effects of the lead-molecule configuration (para, meta, or ortho positions) on transport characteristics of the junction.

The paper is organized as follows. In Sec. II, we introduce the model and formulate the NEGF scheme. Numerical results for inelastic (total and circular) currents are presented and discussed in Sec. III. Section IV concludes and outlines directions for future study.

II. MODEL AND METHOD

We consider a benzene molecule, M , connected to two metal leads, L and R , at either para, meta, or ortho positions. The molecule is described by a tight-binding model with on-site energy α_M and the elastic hopping matrix element β_M . The metal leads are modeled as semi-infinite one-dimensional tight-binding chains with the on-site energy α_K and hopping β_K ($K = L, R$). The leads are reservoirs of free electrons, each at its own thermal equilibrium. Coupling between molecule and leads is characterized by tunneling matrix elements β_{LM}

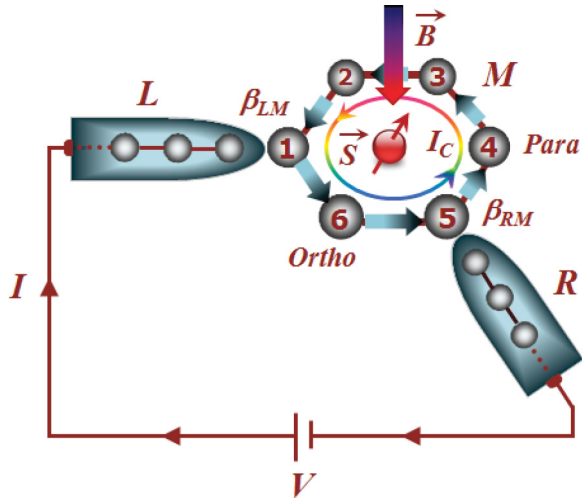


FIG. 1. (Color online) A tight-binding model for current conduction through a molecular ring M with a spin impurity \vec{S} at its center coupled to metal leads L and R in a meta position (sites of ortho and para configurations are indicated in the figure). External uniform magnetic field \vec{B} is applied perpendicular to the ring plane.

and β_{RM} for L - M and R - M interfaces, respectively. An impurity atom with spin \vec{S} is placed at the center of the ring. Following Ref. 67, we disregard dynamics of the local spin, and assume fast thermalization. Figure 1 presents a sketch of the model. The Hamiltonian of the model is (here and below, $|e| = \hbar = m_e = 1$)

$$\hat{H} = \hat{H}_M + \sum_{K=L,R} (\hat{H}_K + \hat{V}_{KM}) + \hat{V}_{SM} \equiv \hat{H}_0 + \hat{V}_{SM}, \quad (1)$$

where \hat{H}_M and \hat{H}_K introduce electronic degrees of freedom in the molecule and in the contact K ($K = L, R$), respectively. \hat{V}_{KM} is coupling between molecule and contact K and \hat{V}_{SM} describes exchange interaction of conduction electrons with the local spin. The explicit expressions are

$$\hat{H}_M = \sum_{m \in M, \sigma} \alpha_M(V_g) \hat{d}_{m\sigma}^\dagger \hat{d}_{m\sigma} + \sum_{(m_1, m_2) \in M, \sigma} (\beta_M \hat{d}_{m_1\sigma}^\dagger \hat{d}_{m_2\sigma} + \text{H.c.}), \quad (2)$$

$$\hat{H}_K = \sum_{k \in K, \sigma} \alpha_K \hat{c}_{k\sigma}^\dagger \hat{c}_{k\sigma} + \sum_{(k_1, k_2) \in K, \sigma} (\beta_K \hat{c}_{k_1\sigma}^\dagger \hat{c}_{k_2\sigma} + \text{H.c.}), \quad (3)$$

$$\hat{V}_{KM} = \sum_{\sigma} (\beta_{KM} \hat{c}_{k\sigma}^\dagger \hat{d}_{m_K\sigma} + \text{H.c.}), \quad (4)$$

$$\hat{V}_{SM} = \sum_{m_1, m_2 \in M, \sigma_1, \sigma_2} J_{m_1 m_2} (\vec{S} \cdot \vec{\sigma}_{\sigma_1 \sigma_2}) \hat{d}_{m_1 \sigma_1}^\dagger \hat{d}_{m_2 \sigma_2}. \quad (5)$$

Here, $\hat{d}_{m\sigma}^\dagger$ ($\hat{d}_{m\sigma}$) and $\hat{c}_{k\sigma}^\dagger$ ($\hat{c}_{k\sigma}$) are the creation (annihilation) operators for an electron of spin σ (\uparrow, \downarrow) at site m in the molecule and site k in the lead, respectively. $\alpha_M(V_g) \equiv \alpha_M + V_g$ is the gated molecular on-site energy (V_g is the gate voltage). \vec{S} is the vector spin operator of the impurity and $\vec{\sigma}_{\sigma_1 \sigma_2}$ is the $\sigma_1 \sigma_2$ matrix element of the vector of Pauli spin matrices $\vec{\sigma} \equiv (\sigma_x, \sigma_y, \sigma_z)$. $\langle i, j \rangle$ indicates that i and j are the nearest neighbors. k_K is the site in the atomic chain in the immediate

neighborhood of the molecular site m_K ($K = L, R$); $m_L = 1$ and $m_R = 5$ for the meta configuration shown in Fig. 1. $J_{m_1 m_2}$ is the spin-spin exchange interaction coupling strength. Below, we consider two types of this interaction: the s - d model,⁷⁸

$$J_{m_1 m_2} = \delta_{m_1, m_2} J, \quad (6a)$$

and the spin-dependent tunneling matrix element model,⁷⁹

$$J_{m_1 m_2} = \delta_{\langle m_1, m_2 \rangle} J. \quad (6b)$$

Here, $\delta_{\langle m_1, m_2 \rangle}$ indicates that m_1 and m_2 are the nearest neighbors.

We note that the molecular Hamiltonian (2) is a standard Pariser-Parr-Pople (PPP) model routinely used in quantum chemistry as a semiempirical quantum-mechanical method for description of conjugated and aromatic hydrocarbons.^{80,81} Note also that spin-spin exchange coupling of the type given in Eq. (5) was employed in a number of theoretical considerations of similar systems.^{64,65,67,82,83}

A static uniform magnetic field \vec{B} is applied perpendicular to the ring plane.⁹⁹ We assume that the field is confined to the molecule region only. In the presence of the field, the on-site energy α_M becomes spin dependent (the Zeeman effect) and the hopping matrix element β_M acquires a phase factor θ :^{46,47}

$$\alpha_{M\sigma} \equiv \alpha_M - 2\mu_B B_{\text{tot}}\sigma, \quad (7)$$

$$\beta_M \rightarrow \beta_M e^{i\theta}, \quad \theta \equiv 2\pi \frac{\phi_{B_{\text{tot}}}}{6\phi_0}, \quad (8)$$

where $\mu_B = e\hbar/2m_e$ is the Bohr magneton, $B_{\text{tot}} \equiv B + B_{\text{ind}}$ is the total magnetic field (external plus current induced), $\phi_0 = h/|e|$ is the flux quantum, and $\phi_{B_{\text{tot}}}$ is the total magnetic flux through the benzene ring. The magnetic field also removes the degeneracy of the local spin eigenstates $|SM_S\rangle$,

$$E_{SM_S} = -2\mu_B B_{\text{tot}} M_S. \quad (9)$$

We assume quick relaxation of the local spin, so that the probability P_{SM_S} for the eigenstates occupations follows the Boltzman distribution. Note that fast thermalization of the local spin is a reasonable approximation as long as the spin-spin exchange is relatively weak and the impurity is strongly coupled to a bath (the latter may be represented, e.g., either by a chain of atoms, or a metallic surface with the impurity chemisorbed on it). This assumption has also been considered in a number of previous studies.^{60–65,67}

The central quantity of interest is the single-particle electronic Green function, defined on the Keldysh contour as

$$G_{m\sigma, m'\sigma'}(\tau, \tau') = -i \langle T_c \hat{d}_{m\sigma}(\tau) \hat{d}_{m'\sigma'}^\dagger(\tau') \rangle, \quad (10)$$

where T_c is the contour ordering operator. Note that in the absence of spin-spin correlations in the zero-order Hamiltonian \hat{H}_0 , Eqs. (2)–(4), and within the SCBA treatment of the spin-spin interaction \hat{V}_{SM} , Eq. (5), the electron Green function (10) is block diagonal in the spin space:¹⁰⁰

$$G_{m\sigma, m'\sigma'}(\tau, \tau') = \delta_{\sigma, \sigma'} G_{mm', \sigma}(\tau, \tau'). \quad (11)$$

It satisfies the Dyson equation

$$\begin{aligned} G_{mm',\sigma}(\tau, \tau') &= G_{mm',\sigma}^{(0)}(\tau, \tau') + \sum_{m_1, m_2 \in M} \int_c d\tau_1 \int_c d\tau_2 G_{mm_1, \sigma}^{(0)}(\tau, \tau_1) \\ &\quad \times \sum_{m_1, m_2, \sigma}^{(S)}(\tau_1, \tau_2) G_{m_2 m', \sigma}(\tau_2, \tau'), \end{aligned} \quad (12)$$

where $G_{mm',\sigma}^{(0)}$ is the electron Green function in the absence of the spin-spin exchange interaction \hat{V}_{SM} , Eq. (5), and $\Sigma_{m_1, m_2, \sigma}^{(S)}$ is the electron self-energy due to this interaction. Note that the free-electron Green function $G_{mm',\sigma}^{(0)}$ incorporates self-energies due to coupling to the contacts (see Appendix A for details),

$$\Sigma_{m_1, m_2, \sigma}^{(K)}(\tau_1, \tau_2) = \delta_{m_1, m_K} \delta_{m_2, m_K} |\beta_{KM}|^2 g_{k_K, \sigma}(\tau_1, \tau_2), \quad (13)$$

where $g_{k_K, \sigma}(\tau_1, \tau_2) \equiv -i \langle T_c \hat{c}_{k_K \sigma}(\tau_1) \hat{c}_{k_K \sigma}^\dagger(\tau_2) \rangle$ is the surface Green function of the contact K . Note also that the Dyson equation in the form of Eq. (12) is valid only within the noncrossing approximation.⁸⁵ Indeed, Eq. (12) assumes that the coupling to contacts, see Eq. (4), and spin-spin exchange, see Eq. (5), contribute additively to the total electron self-energy.

The spin-spin exchange interaction (5) is treated within the SCBA. The corresponding expression for the self-energy is (see Appendix B for derivation)

$$\begin{aligned} \Sigma_{m_1, m_2, \sigma}^{(S)}(\tau_1, \tau_2) &= \delta(\tau_1, \tau_2) \Sigma_{m_1, m_2, \sigma}^{(S)\delta} \\ &\quad + \Sigma_{m_1, m_2, \sigma}^{(S)\text{el}}(\tau_1, \tau_2) + \Sigma_{m_1, m_2, \sigma}^{(S)\text{inel}}(\tau_1, \tau_2), \end{aligned} \quad (14)$$

where

$$\Sigma_{m_1, m_2, \sigma}^{(S)\delta} = J_{m_1 m_2} \sigma \sum_{M_S} P_{SM_S} M_S, \quad (15)$$

$$\begin{aligned} \Sigma_{m_1, m_2, \sigma}^{(S)\text{el}}(\tau_1, \tau_2) &= \sum_{m_3, m_4 \in M} J_{m_1 m_3} G_{m_3 m_4, \sigma}(\tau_1, \tau_2) J_{m_4 m_2} \\ &\quad \times \sum_{M_S} P_{SM_S} (1 - P_{SM_S}) M_S^2, \end{aligned} \quad (16)$$

$$\begin{aligned} \Sigma_{m_1, m_2, \sigma}^{(S)\text{inel}}(\tau_1, \tau_2) &= \sum_{m_3, m_4 \in M} J_{m_1 m_3} G_{m_3 m_4, \sigma}(\tau_1, \tau_2) J_{m_4 m_2} \\ &\quad \times \sum_{M_S, M_S' (|M_S - M_S'|=1)} B_{M_S}(\tau_1, \tau_2) B_{M_S'}(\tau_2, \tau_1), \\ &\quad \times \frac{(S + \xi M_S)(S - \xi M_S + 1)}{2} (1 - \xi \sigma) \end{aligned} \quad (17)$$

with $\xi \equiv \text{sgn}(M_S - M_S')$, $\bar{\sigma} \equiv -\sigma$, and

$$B_{M_S}(\tau_1, \tau_2) \equiv i [P_{SM_S} - \theta_C(\tau_1, \tau_2)] e^{-iE_{SM_S}(t_1 - t_2)}. \quad (18)$$

Here, $\theta_C(\dots)$ is the Heaviside step function defined on the contour, and $t_{1,2}$ are the real times corresponding to the $\tau_{1,2}$ contour variables. Equations (12) and (14) are then solved self-consistently. The self-consistency results from the interdependence of the Green function, self-energy, and magnetic field induced by a circular current in the ring.

The converged Green function (11) is used to calculate currents in the molecule. In particular, within the same effective second-order perturbative expansion in \hat{V}_{SM} , the spin-resolved molecular bond current is (see Appendix C for

derivation)

$$I_{m_1 \rightarrow m_2}^\sigma(t) \approx \frac{2e}{\hbar} \text{Re}[\beta_{m_1, m_2, \sigma} G_{m_2 m_1, \sigma}^<(t, t)], \quad (19)$$

where

$$\beta_{m_1, m_2, \sigma} \equiv \beta_M + \Sigma_{m_1, m_2, \sigma}^{(S)\delta} \quad (20)$$

with m_1, m_2 , the nearest-neighboring sites.

Following Ref. 75, we can write an approximate expression for the spin-resolved circular current (see Appendix C for a short discussion):

$$I_c^\sigma(t) \approx \sum_{\langle m_1, m_2 \rangle \in M} I_{m_1 \rightarrow m_2}^\sigma(t) \frac{\ell_{\langle m_1, m_2 \rangle}}{L}. \quad (21)$$

Here, counterclockwise direction is taken as positive (see Fig. 1), the sum is over all bonds of the molecular ring, $\ell_{\langle m_1, m_2 \rangle}$ is the length of the bond $\langle m_1, m_2 \rangle$ (here length of the C-C bond in benzene is 1.4 Å) and $L \equiv \sum_{\langle m_1, m_2 \rangle \in M} \ell_{\langle m_1, m_2 \rangle}$.

The spin-resolved current at the molecule-contact interface K is⁸⁸

$$\begin{aligned} I_K^\sigma(t) &= \frac{2e}{\hbar} \sum_{m_1, m_2 \in M} \text{Re} \int_{-\infty}^t dt_1 [\Sigma_{m_1, m_2, \sigma}^{(K)<}(t, t_1) G_{m_2 m_1, \sigma}^>(t_1, t) \\ &\quad - \Sigma_{m_1, m_2, \sigma}^{(K)>}(t, t_1) G_{m_2 m_1, \sigma}^<(t_1, t)]. \end{aligned} \quad (22)$$

Our consideration below is restricted to steady-state, where projections of the electron Green function (11) and self-energies (13) and (14) depend only on a time difference, thus it is convenient to make the Fourier transformation to energy space. Currents (21) and (22) are time independent, and the current at the interface K is given by the Kirchhoff's law as a sum of currents in bonds connected to the site m_K . Note, however, that circular current expression (21) is approximate, while expression for the terminal current (22) is exact. Thus *a priori* there is no guarantee that the Kirchhoff's law is strictly fulfilled even when GFs in these expressions are evaluated within a conserving approximation.

In summary, Eqs. (12) and (14) set up a self-consistent procedure at the SCBA level. Converged results are utilized in Eqs. (21) and (22) to calculate circular and terminal currents, respectively.

III. RESULTS AND DISCUSSION

We now present results of steady-state simulations of the circular and terminal currents for the model (1)–(5) with local spin chosen as $S = 1$. Unless stated otherwise, parameters for the calculations are $T = 0.5$ K, $\alpha_M = -2$ eV and $\beta_M = 2.5$ eV, $\alpha_K = 0$ and $\beta_K = 6$ eV ($K = L, R$), $\beta_{LM} = \beta_{RM} = 0.3$ eV, and $J = 5$ meV. For these parameters, the electron escape rate due to coupling to contacts is $\Gamma_K = 2|\beta_{KM}|^2/|\beta_K| = 30$ meV. The Fermi energy is taken in the middle of the conduction band, $E_F = 0$, and the bias V is applied symmetrically $\mu_{L,R} = E_F \pm V/2$. Calculations are performed on an energy grid spanning the range from -1.5 to 1.5 eV in steps of 10^{-5} eV.

We note that the parameters are chosen to represent a realistic molecular junction. In particular, the hopping matrix element β_M is chosen to represent the carbon-carbon bond in

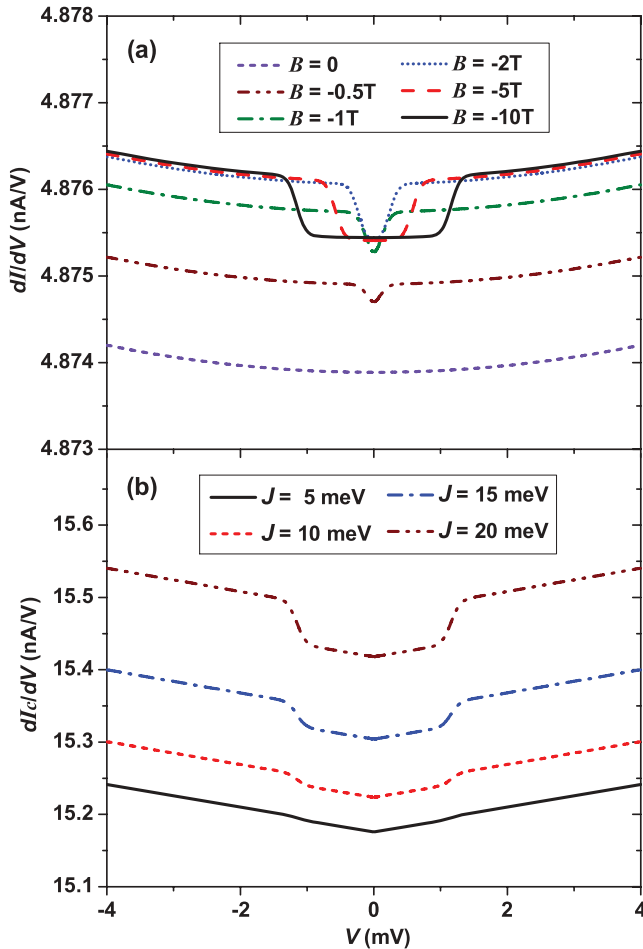


FIG. 2. (Color online) Inelastic transport in a meta-connected benzene ring molecular junction. Shown are (a) conductance dI/dV ($I_L = I_R \equiv I$) vs bias for several magnetic field strengths (negative B represents a field pointing into the plane of the ring) and (b) circular conductance dI_C/dV vs bias at $B = -10$ T for several values of electron-spin exchange parameter J .

benzene within the PPP model.^{80,95} The onsite energy α_M is chosen to set the lowest unoccupied molecular orbital (LUMO) at ~ 0.5 eV above the Fermi in the metal following Ref. 96.¹⁰¹ The unphysically large value of hopping matrix element β_K we consider for contacts is just a way to enforce the wide-band limit (bandwidth 24 eV). The onsite energy in contacts α_K defines origin of the energy scale. Strength of molecule-contacts coupling β_{KM} is not well controlled in realistic junctions, and may change by up to three orders of magnitude for the same device depending on experimental setup (compare, for example, experimental data on the benzenedithiol molecular junction reported in Refs. 97 and 8). Thus we choose these parameters utilizing data of Ref. 67. Interestingly, results for conductance in the low-bias region obtained with these parameters (see Fig. 2) are in agreement with the experimental data reported in Ref. 8. Finally, spin-spin exchange coupling parameter J is taken within the range considered in similar previous studies.^{82,83}

The self-consistent iterations of Eqs. (12) and (14) are performed till currents (19)–(22) are converged with a tolerance of 0.01%. We note in passing that for the chosen parameters

both models (6) yield qualitatively similar results. Below, we present results of calculations for the tunneling model (6b). Note also that for these parameters currents calculated using Eq. (22) and as a sum of bond currents at the junction (the Kirchhoff's law) are identical.

First, we present inelastic features in the total current $I_L = -I_R \equiv I$, Eq. (22), for a meta connected benzene ring molecular junction (results for the para- and ortho-connected rings are qualitatively similar). Figure 2(a) depicts the conductance (dI/dV) at low bias for several values of applied magnetic field B . The conductance step, an indication of opening of an inelastic channel, demonstrates linear shift towards higher voltages with increase of the magnetic field strength. The effect is due to increase of level separation in the local spin system, Eq. (9). Note that the field reversal, $B \rightarrow -B$, does not affect the conductance spectra. Results presented in Fig. 2(a) are similar to experimental data,^{56–58} where spin-flip IETS was observed for atomic structures studied with STM, and corresponding theoretical simulations.^{60,64–67}

Inelastic effects are observed also in circular current. Figure 2(b) shows circular conductance at low bias for several spin-exchange coupling strengths. As expected, stronger inelastic coupling strength results in a more pronounced step in the conductance. Note steeper increase of circular compared to total current [note, the solid curve in Fig. 2(a) is calculated for the same parameters as in Fig. 2(b)]. This can be understood by considering that for a small molecule-contact coupling electrons entering the ring spend a long time circulating in the ring, before being escaped to the other terminal,⁹¹ which results in large circular currents in the ring.

Note that the IETS signal presented in Fig. 2, in principle, should be observable also for $B = 0$ due to the magnetic field induced by the circular current. However, realistic estimate of the induced field yields $B_{\text{ind}} \sim 0.2$ T, which results in splitting of spin states of the local impurity of the order of 0.01 meV. Thus observation of inelastic effects in the absence of external magnetic field is not feasible.

The renormalization of elastic scattering with opening of inelastic channel may lead to either increase or decrease of the total current (step up or down in the conductance) at the threshold.⁹² Previous considerations,^{60,63–65,67} which employed lowest-order perturbation theory, have not accounted for the renormalization of the elastic channel. For a model of single molecular level ε_0 coupled to a single molecular vibration, the change in conductance near the threshold is proportional to [see Eq. (36) in Ref. 92]

$$\frac{[\mu - \varepsilon_0 - \text{Re} \Sigma_{\text{inel}}^r(\mu)]^2 - (\Gamma/2)^2}{[\mu - \varepsilon_0 - \text{Re} \Sigma_{\text{inel}}^r(\mu)]^2 + (\Gamma/2)^2}, \quad (23)$$

where μ is electrochemical potential and Σ_{inel}^r is retarded projection of the self-energy due to coupling to molecular vibration. Thus transition between the two features in vibrational IETS can be achieved either by applying gate voltage (i.e., changing $\mu - \varepsilon_0$) or equivalently by changing strength of the molecule-contacts coupling Γ (e.g., in STM experiment). Figure 3(a) demonstrates this transition for spin-flip IETS of the model (1)–(5).

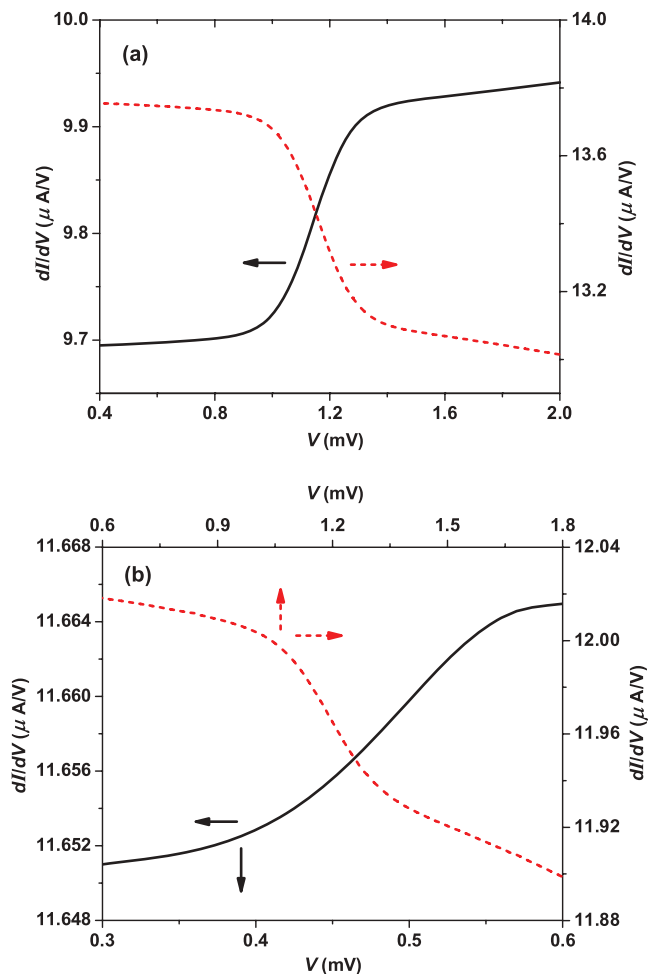


FIG. 3. (Color online) Elastic channel renormalization in a meta-connected benzene ring molecular junction. Shown is conductance dI/dV ($I_L = I_R \equiv I$) vs bias (a) at $B = -10$ T for two different values of gate voltage: $V_g = 0.486$ V (solid line, black) and 0.490 V (dashed line, red); (b) at $V_g = 0.488$ V for two different values of applied magnetic field: $B = -5$ T (solid line, black; left and bottom axes) and -10 T (dashed line, red; right and top axes).

Contrary to vibrational spectroscopy, where the inelastic channel threshold is set by the frequency of vibration, the excitation energy of a spin inelastic process can be adjusted by a magnetic field. This allows tuning of the corresponding self-energy [see, e.g., Σ_{inel}^r in Eq. (23)]. Figure 3(b) shows control of conductance behavior at the threshold by an external magnetic field.

Peaks and dips in IETS spectrum were observed experimentally in vibrational IETS measurements (see, e.g., Refs. 11 and 93) and should be expected also in the spin-flip IETS. Since an external magnetic field is a simpler control than either a gate potential or molecule-contacts coupling strength, observation of transition between the two types of the IETS signal should be easier for spin-flip IETS.

We now turn to the resonant tunneling regime with LUMO entering the bias window at $V \sim 1$ V. Spin-spin exchange coupling V_{SM} , see Eq. (5), induces spin-dependent

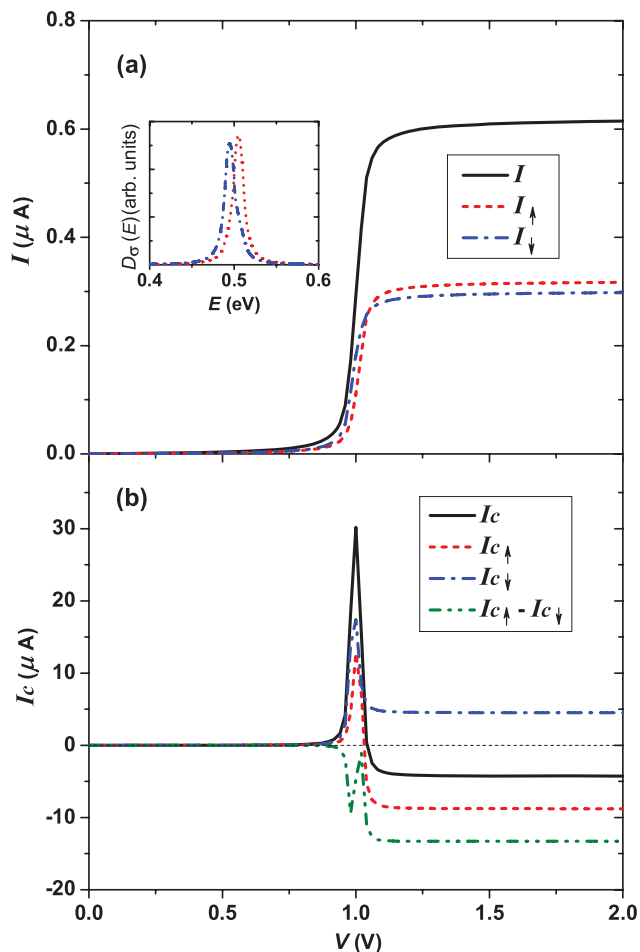


FIG. 4. (Color online) Current-voltage characteristics of a meta-connected molecular ring junction. Shown are (a) terminal current $I_L = I_R \equiv I$, Eq. (22), and (b) circular current I_c , Eq. (21), at $B = -5$ T for spin-up (dashed line, red), spin-down (dash-dotted line, blue), total charge (solid line, black), and total spin (dash-double-dotted line, green) currents. The inset in (a) shows the spin resolved local density of states $D_{\sigma}(E)$, Eq. (24), at $V = 1$ V (spin-up - dashed line, red, spin-down - dash-dotted line, blue)

renormalization of the local density of states:

$$D_{\sigma}(E) \equiv -\frac{1}{\pi} \text{Im Tr}[G_{\sigma}^r(E)]. \quad (24)$$

Figure 4(a) shows terminal current $I_L = -I_R \equiv I$, see Eq. (22), as a function of bias. The spin polarization at the resonant threshold, $V \sim 1$ V, is due to splitting of the local density of states (see inset in the Fig. 4).

The effect of the renormalization is even more drastic for circular current [see Fig. 4(b)]. Here, the polarization above the threshold differs qualitatively: spin-up and spin-down components move in opposite directions (compare dashed and dash-dotted lines). As a result, the circular charge current is suppressed while simultaneously a large spin circular current is observed in the ring. The effect can be understood in terms of orbital momentum states (degenerate for an isolated ring) represented by Bloch waves going in opposite directions. As discussed in Ref. 75, molecule-contacts coupling removes this degeneracy. In the presence of the spin-spin exchange

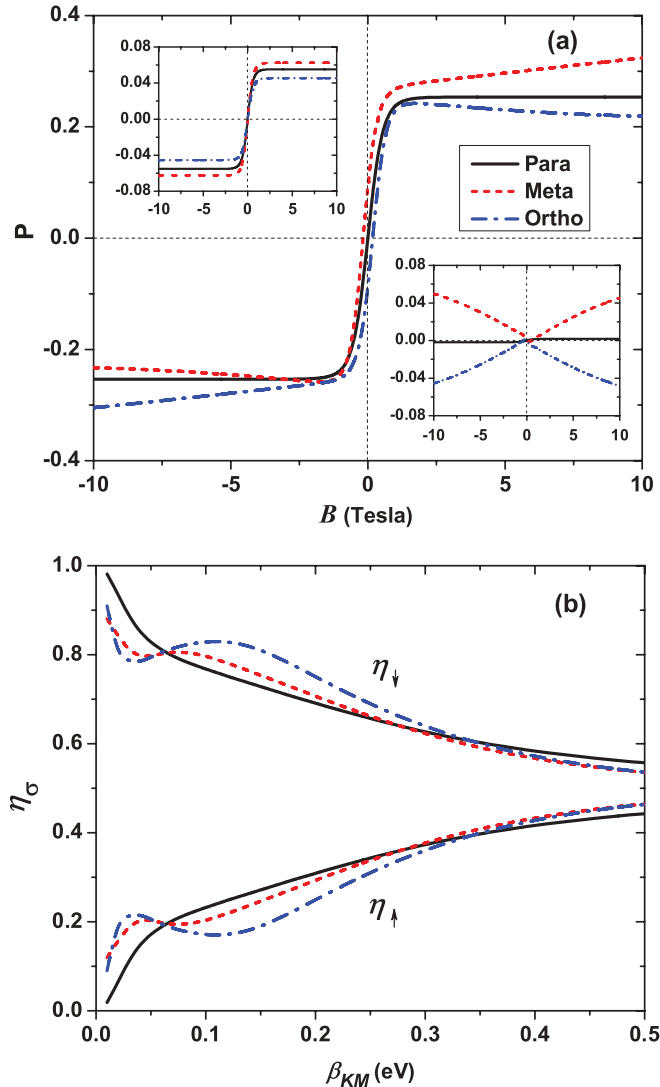


FIG. 5. (Color online) Spin-polarized transport in the para (solid line, black), meta (dashed line, red), and ortho (dash-dotted line, blue) connected molecular ring junctions. Shown are: (a) Spin polarization P , Eq. (25), as a function of applied magnetic field for at resonant bias ($V = 1$ V), and (b) spin filter efficiency η_σ , Eq. (25), as function of the molecule-contacts coupling strength. Insets in (a) show spin polarization for bias below ($V = 0.8$ V, upper inset) and above ($V = 1.2$ V, lower inset) the resonance.

interaction, the corresponding states appear to be spin polarized [see inset in Fig. 4(a)]. It is interesting to note that in contrast to the symmetrically connected ring that lacks biased induced circular current and the associated magnetic field, the spin-resolved currents in the asymmetrically connected rings remain split around 1 V bias even when the applied field is removed due to the magnetic field induced by a circular current.

The possibility of an experimental detection of the charge circular current at resonant threshold by measuring the current-induced magnetic field was discussed in Ref. 75. Presence of spin-spin exchange interaction yields almost pure spin circular current above the threshold. In principle, the spin circular current may be measurable by, e.g., detecting its induced

electric field as discussed in Ref. 94, however, we are not aware of experimental feasibility of such a measurement.

To delve further into the spin-resolved currents in the rings, we define the spin polarization of the total current as

$$P = (I_\uparrow - I_\downarrow)/(I_\uparrow + I_\downarrow) \equiv \eta_\uparrow - \eta_\downarrow, \quad (25)$$

where $\eta_\sigma \equiv I_\sigma/I$ is the spin filter efficiency. Figure 5(a) shows spin polarization in the ring with leads at para, meta, and ortho positions for a bias voltage tuned for level resonance transmission. The insets depict polarizations at bias above and below 1 V. Several points are noteworthy. First, the polarization at resonant bias is far larger than that at off-resonant bias. Second, the asymmetrically connected rings offer better control of spin-resolved currents over a symmetrically connected ring. Third, the renormalization in the density of states (in particular, which spin projection has a peak at lower energy) dictates a change of sign of the polarization with the field reversal. Fourth, positive polarization for meta (negative for ortho) coupling above the resonance irrespective of the sign of the magnetic field indicates a leading role of interference effect induced by phase θ , see Eq. (8), rather than the renormalization of the local density in this regime.

Figure 5(b) shows spin filter efficiency as a function of strength of molecule-contacts coupling. As expected, the stronger coupling between the ring and paramagnetic contacts reduces spin selectivity. Nonmonotonic behavior for meta and ortho and fast drop in polarization for para coupled ring at weak coupling strengths, $\beta_{KM} \sim 0.05$ eV, indicate presence of inelastic (spin-flip) effects, which are pronounced at $\Gamma \sim J$.

Note that the terminal current polarization is easily measurable experimentally. Inelastic effects are of secondary importance here (although they are pronounced for weak molecule-contacts coupling). We note that the use of benzene-substituted organic molecules as spin-filter devices has recently been discussed in the literature.⁵¹ We see that the effect is robust with respect to decoherence, and is sensitive to the topology of the molecule-contact coupling, which indicates a possibility of coherently controlled molecular electronics.

IV. CONCLUSIONS

We present a study of spin inelastic currents in molecular ring junctions. Within a simple model of a benzene molecule coupled to paramagnetic contacts at meta, ortho, and para positions, we discuss the role of external magnetic field and local spin impurity placed at the center of the ring on spin-flip IETS and the spin polarization of circular and total currents.

Our study extends recent considerations of spin-flip IETS^{60–67} formulating a conserving approximation applicable to multisite molecular systems. It also takes into account the renormalization of elastic scattering channel, which is known to cause a qualitative change in the IETS signal.

This work is also an extension of recent studies of circular currents in molecular junctions.^{46,47,75} Our NEGF formulation allows to go beyond previous scattering theory considerations. The main results of the study are the following: (a) like

vibrational also spin-flip IETS yields the possibility of control of the IETS signal. Moreover, in addition to gate bias and molecule-contacts coupling strength, also magnetic field can be used as a control of the spin-flip IETS spectrum. This feature should be measurable in any junction with spin-spin exchange interaction. (b) The spin-spin exchange interaction in ring structures results in spin circular currents. The effect, in principle, is detectable by measuring current-induced electric fields.⁹⁴ (c) Molecular ring structures may be used as sources of spin-polarized terminal currents. Note that recently benzene substituted organic molecules have been proposed as molecular spin filters.⁵¹ Here, we demonstrate that the effect is robust with respect to decoherence, and is sensitive to topology of the molecule-contact coupling.

Although our consideration is restricted to a simple theoretical model, the effects should be observable experimentally. Indeed, we discuss two types of effects: (a) those related to inelastic transport and (b) spin polarization due to coherence in the molecule. First, the opening of an inelastic channel is a robust effect observed (in the case of vibrational IETS) in many experimental studies (see, e.g., Refs. 11 and 93). In this respect, experimental observation of the spin-flip IETS is similar to those of the vibrational inelastic electron spectroscopy. Second, the spin polarization of terminal currents is caused by the presence of a molecular ring. Effects of coherence related to ring molecular structures in junctions have been observed experimentally in Refs. 36 and 37. Also, recently, similar spin polarization in helical molecular junctions was reported in Ref. 98. An extension of the study to *ab initio* simulations of transport in similar structures will be considered in future research.

ACKNOWLEDGMENTS

We gratefully acknowledge support by the National Science Foundation (CHE-1057930), the US-Israel Binational Science Foundation (Grant No. 2008282), and the Hellman Family Foundation.

APPENDIX A: ELECTRON SELF-ENERGY DUE TO COUPLING TO CONTACTS

For the model of semi-infinite atomic chain, Eq. (3), retarded, lesser, and greater projections⁸⁶ of the self-energy (13) in energy space,

$$\Sigma_{m_1 m_2, \sigma}^{(K)r}(E) = \delta_{m_1, m_K} \delta_{m_2, m_K} \left[\Lambda_K(E) - \frac{i}{2} \Gamma_K(E) \right], \quad (\text{A1})$$

$$\Sigma_{m_1 m_2, \sigma}^{(K)<}(E) = i \delta_{m_1, m_K} \delta_{m_2, m_K} \Gamma_K(E) f_K(E), \quad (\text{A2})$$

$$\Sigma_{m_1 m_2, \sigma}^{(K)>}(E) = -i \delta_{m_1, m_K} \delta_{m_2, m_K} \Gamma_K(E) [1 - f_K(E)], \quad (\text{A3})$$

are expressed in terms of the Newns-Anderson formula:⁸⁷

$$\Lambda_K(E) = \frac{|\beta_{KM}|^2}{|\beta_K|} \begin{cases} \epsilon + \sqrt{\epsilon^2 - 1}, & \epsilon < -1, \\ \epsilon, & |\epsilon| \leq 1, \\ \epsilon + \sqrt{\epsilon^2 - 1}, & \epsilon > 1, \end{cases} \quad (\text{A4})$$

$$\Gamma_K(E) = \frac{2|\beta_{KM}|^2}{|\beta_K|} \begin{cases} \sqrt{1 - \epsilon^2}, & |\epsilon| \leq 1, \\ 0, & \text{otherwise.} \end{cases} \quad (\text{A5})$$

Here, $\epsilon \equiv (E - \alpha_K)/|2\beta_K|$ and $f_K(E)$ is the Fermi-Dirac distribution.

APPENDIX B: ELECTRON SELF-ENERGY DUE TO SPIN-SPIN EXCHANGE INTERACTION

In the definition of the single-electron Green function (10), operators $\hat{d}_{m\sigma}(\tau)$ and $\hat{d}_{m'\sigma'}^\dagger(\tau')$ are in the Heisenberg representation. Transforming this expression to the interaction representation with respect to the zero-order Hamiltonian \hat{H}_0 , Eq. (1), yields

$$G_{m\sigma, m'\sigma'}(\tau, \tau') = -i \langle T_c \hat{d}_{m\sigma}(\tau) \hat{d}_{m'\sigma'}^\dagger(\tau') e^{-i \int_c d\tau_1 \hat{V}_{SM}^I(\tau_1)} \rangle_0, \quad (\text{B1})$$

where $\hat{V}_{SM}^I(\tau_1)$ is operator of the spin-spin exchange interaction (5) in the interaction representation, and subscript 0 indicates evolution governed by the zero-order Hamiltonian. Expanding the exponent in Eq. (B1) up to second order in \hat{V}_{SM}^I , collecting and dressing connected diagrams in the expansion,⁸⁵ leads to the Dyson equation with self-energy

$$\begin{aligned} \Sigma_{m_1 \sigma_1, m_2 \sigma_2}^{(S)}(\tau_1, \tau_2) &= \delta(\tau_1, \tau_2) J_{m_1 m_2} \langle \hat{O}_{\sigma_1 \sigma_2}(\tau_1) \rangle_S \\ &+ \sum_{\substack{m'_1, m'_2 \in M \\ \sigma'_1, \sigma'_2}} J_{m_1 m'_1} G_{m'_1 \sigma'_1, m'_2 \sigma'_2}(\tau_1, \tau_2) J_{m'_2 m_2} \\ &\times \langle T_c \hat{O}_{\sigma_1 \sigma'_1}(\tau_1) \hat{O}_{\sigma'_2 \sigma_2}(\tau_2) \rangle_S. \end{aligned} \quad (\text{B2})$$

Here,

$$\hat{O}_{\sigma_1 \sigma_2}(\tau_1) \equiv \hat{S}(\tau_1) \cdot \vec{\sigma}_{\sigma_1 \sigma_2}, \quad (\text{B3})$$

$\vec{\sigma}$ is vector of the Pauli matrices and $\langle \dots \rangle_S$ indicates average over the equilibrium distribution of the local spin system.

Following Ref. 67, we rewrite the operator \hat{S} as

$$\hat{S}(\tau) = \sum_{M_S, M'_S} \langle SM'_S | \hat{S} | SM_S \rangle \hat{b}_{M'_S}^\dagger(\tau) \hat{b}_{M_S}(\tau) \quad (\text{B4})$$

with $\hat{b}_{M'_S}^\dagger$ and \hat{b}_{M_S} assumed to be Fermi operators, and introduce quasiparticle Green function

$$B_{M_S M'_S}(\tau, \tau') \equiv -i \langle T_c \hat{b}_{M_S}(\tau) \hat{b}_{M'_S}^\dagger(\tau') \rangle, \quad (\text{B5})$$

which for unperturbed equilibrium local spin system takes the form of Eq. (18).

Substituting Eq. (B4) into Eq. (B2), taking into account that zero-order Hamiltonian does not contain spin-flip processes, and utilizing Eq. (18) and⁸⁹

$$\begin{aligned} \langle SM'_S | \hat{S} | SM_S \rangle &= \delta_{M'_S, M_S} \vec{e}_z \hbar M_S + \delta_{M'_S, M_S \pm 1} (\vec{e}_x \mp i \vec{e}_y) \frac{\hbar}{2} \\ &\times \sqrt{(S \mp M_S)(S \pm M_S + 1)} \end{aligned} \quad (\text{B6})$$

leads to Eqs. (14)–(17).

APPENDIX C: BOND CURRENT

To derive an expression for the bond current, we start from the equation of motion for the spin-resolved population at site m_1 :

$$-\frac{d}{dt} \langle \hat{n}_{m_1 \sigma}(t) \rangle = -\frac{i}{\hbar} \langle [\hat{H}; \hat{n}_{m_1}(t)] \rangle$$

$$= \frac{2}{\hbar} \text{Re} \sum_{m_2 \in M, \sigma'} (\delta_{(m_1, m_2)}) \beta_M G_{m_2 \sigma', m_1 \sigma}^<(t, t) + i J_{m_1 m_2} (\hat{O}_{\sigma \sigma'}(t) \hat{d}_{m_1 \sigma}^\dagger(t) \hat{d}_{m_2 \sigma'}(t)), \quad (\text{C1})$$

where $\hat{n}_m \equiv \hat{d}_m^\dagger \hat{d}_m$, $\hat{O}_{\sigma \sigma'}$ is defined in Eq. (B3), and we used Eqs. (1)–(5).

Each term in the sum in the right of Eq. (C1) is a flux from site m_2 to site m_1 . Utilizing Eq. (11), expanding the last term in the right of Eq. (C1) up to second order in the spin-spin exchange interaction (5), and neglecting contribution from m_2 beyond the nearest-neighbor sites¹⁰² leads to Eq. (19) for the bond current.

Reference 75 introduces a circular current as the sole source of flux through a ring, employing the Biot-Savart expression for time-independent current in the derivations. The time-dependent generalization of the Biot-Savart law is

known as Jefimenko's equation:⁹⁰

$$\vec{B}(\vec{r}, t) = \frac{\mu_0}{4\pi} \int d\vec{r}_1 \left\{ \left[\left(\vec{J}(\vec{r}_1, t_1) \right)_{\text{ret}} \times \frac{\vec{R}}{R^3} \right] + \left[\left(\frac{\partial \vec{J}(\vec{r}_1, t_1)}{\partial t_1} \right)_{\text{ret}} \times \frac{\vec{R}}{cR^2} \right] \right\}, \quad (\text{C2})$$

where $\vec{R} \equiv \vec{r} - \vec{r}_1$ and $(f(\vec{r}_1, t_1))_{\text{ret}} \equiv f(\vec{r}_1, t - R/c)$. Since the characteristic distance for benzene ring is $R \sim 1.4 \text{ \AA}$, the retardation effect is confined to times of the order of $R/c \sim 10^{-18} \text{ s}$, which may be safely disregarded for currents in molecular junctions. Similarly, the second term in Eq. (C2) can be dropped. This results in an expression that has the form of the usual Biot-Savart law, but with the time-dependent current in it. Under these assumptions, the results of Ref. 75 can be utilized to introduce an expression for the time-dependent circular current as given by Eq. (21).

*dhrai@ucsd.edu

†micalgalperin@ucsd.edu

¹A. Aviram and M. A. Ratner, *Chem. Phys. Lett.* **29**, 277 (1974).

²A. Nitzan and M. A. Ratner, *Science* **300**, 1384 (2003).

³N. J. Tao, *Nat. Nanotechnology* **1**, 173 (2006).

⁴S. M. Lindsay and M. A. Ratner, *Adv. Mat.* **19**, 23 (2007).

⁵M. Galperin, M. A. Ratner, A. Nitzan, and A. Troisi, *Science* **319**, 1056 (2008).

⁶M. A. Reed, C. Zhou, C. J. Muller, T. P. Burgin, and J. M. Tour, *Science* **278**, 252 (1997).

⁷B. Xu and N. J. Tao, *Science* **301**, 1221 (2003).

⁸E. Lortscher, H. B. Weber, and H. Riel, *Phys. Rev. Lett.* **98**, 176807 (2007).

⁹H. Park, J. Park, A. K. L. Lim, E. H. Anderson, A. P. Alivisatos, and P. L. McEuen, *Nature (London)* **407**, 57 (2000).

¹⁰N. B. Zhitenev, H. Meng, and Z. Bao, *Phys. Rev. Lett.* **88**, 226801 (2002).

¹¹R. H. M. Smit, Y. Noat, C. Untiedt, N. D. Lang, M. C. van Hemert, and J. M. van Ruitenbeek, *Nature (London)* **419**, 906 (2002).

¹²P. Kim, L. Shi, A. Majumdar, and P. L. McEuen, *Phys. Rev. Lett.* **87**, 215502 (2001).

¹³B. J. LeRoy, S. G. Lemay, J. Kong, and C. Dekker, *Nature (London)* **432**, 371 (2004).

¹⁴P. Reddy, S.-Y. Jang, R. A. Segalman, and A. Majumdar, *Science* **315**, 1568 (2007).

¹⁵A. Nitzan, *Science* **317**, 759 (2007).

¹⁶Z. Wang, J. A. Carter, A. Lagutchev, Y. K. Koh, N.-H. Seong, D. G. Cahill, and D. D. Dlott, *Science* **317**, 787 (2007).

¹⁷J. A. Carter, Z. Wang, H. Fujiwara, and D. D. Dlott, *J. Phys. Chem. A* **113**, 12105 (2009).

¹⁸J. A. Malen, S. K. Yee, A. Majumdar, and R. A. Segalman, *Chem. Phys. Lett.* **491**, 109 (2010).

¹⁹D. Djukic and J. M. van Ruitenbeek, *Nano Lett.* **6**, 789 (2006).

²⁰M. Tsutsui, M. Taniguchi, and T. Kawai, *Nat. Commun.* **1**, 138 (2010).

²¹M. Kumar, R. Avriller, A. L. Yeyati, and J. M. van Ruitenbeek, *Phys. Rev. Lett.* **108**, 146602 (2012).

²²S. W. Wu, G. V. Nazin, and W. Ho, *Phys. Rev. B* **77**, 205430 (2008).

²³Z. Ioffe, T. Shamai, A. Ophir, G. Noy, I. Yutsis, K. Kfir, O. Cheshnovsky, and Y. Selzer, *Nat. Nanotechnology* **3**, 727 (2008).

²⁴D. R. Ward, N. J. Halas, J. W. Ciszek, J. M. Tour, Y. Wu, P. Nordlander, and D. Natelson, *Nano Lett.* **8**, 919 (2008).

²⁵H. P. Yoon, M. M. Maitani, O. M. Cabarcos, L. Cai, T. S. Mayer, and D. L. Allara, *Nano Lett.* **10**, 2897 (2010).

²⁶D. R. Ward, D. A. Corley, J. M. Tour, and D. Natelson, *Nat. Nanotechnology* **6**, 33 (2011).

²⁷J. R. Petta, S. K. Slater, and D. C. Ralph, *Phys. Rev. Lett.* **93**, 136601 (2004).

²⁸M. Urdampilleta, S. Klyatskaya, J.-P. Cleuziou, M. Ruben, and W. Wernsdorfer, *Nat. Mater.* **10**, 502 (2011).

²⁹S. Sanvito, *Chem. Soc. Rev.* **40**, 3336 (2011).

³⁰A. R. Rocha, V. M. Garcia-suarez, S. W. Bailey, C. J. Lambert, J. Ferrer, and S. Sanvito, *Nat. Mater.* **4**, 335 (2005).

³¹S. Sanvito and A. Rocha, *J. Comput. Theor. Nanosci.* **3**, 624 (2006).

³²L. Bogani and W. Wernsdorfer, *Nat. Mat.* **7**, 179 (2008).

³³S. Sanvito, *Nat. Phys.* **6**, 562 (2010).

³⁴W. Wernsdorfer, *J. Nanotechnology* **7**, 497 (2010).

³⁵J. Fransson and M. Galperin, *Phys. Rev. B* **81**, 075311 (2010).

³⁶C. Patoux, C. Coudret, J.-P. Launay, C. Joachim, and A. Gourdon, *Inorg. Chem.* **36**, 5037 (1997).

³⁷M. Mayor, H.-B. Weber, J. Reichert, M. Elbing, C. von Hänisch, D. Beckmann, and M. Fischer, *Angew. Chem., Int. Ed.* **47**, 5834 (2003).

³⁸H. Lee, Y.-C. Cheng, and G. R. Fleming, *Science* **316**, 1462 (2007).

³⁹S. Kohler, J. Lehmann, and P. Hanggi, *Phys. Rep.* **406**, 379 (2005).

⁴⁰D. M. Cardamone, C. A. Stafford, and S. Mazumdar, *Nano Lett.* **6**, 2422 (2006).

⁴¹S.-H. Ke, W. Yang, and H. U. Baranger, *Nano Lett.* **8**, 3257 (2008).

⁴²Z. Qian, R. Li, X. Zhao, S. Hou, and S. Sanvito, *Phys. Rev. B* **78**, 113301 (2008).

⁴³T. Hansen, G. C. Solomon, D. Q. Andrews, and M. A. Ratner, *J. Chem. Phys.* **131**, 194704 (2009).

⁴⁴G. C. Solomon, C. Herrmann, T. Hansen, V. Mujica, and M. A. Ratner, *Nat. Chem.* **2**, 223 (2010).

- ⁴⁵U. Peskin and M. Galperin, *J. Chem. Phys.* **136**, 044107 (2012).
- ⁴⁶D. Rai, O. Hod, and A. Nitzan, *J. Phys. Chem. Lett.* **2**, 2118 (2011).
- ⁴⁷D. Rai, O. Hod, and A. Nitzan, *Phys. Rev. B* **85**, 155440 (2012).
- ⁴⁸G. Cohen, O. Hod, and E. Rabani, *Phys. Rev. B* **76**, 235120 (2007).
- ⁴⁹C. Herrmann, G. C. Solomon, and M. A. Ratner, *J. Am. Chem. Soc.* **132**, 3682 (2010).
- ⁵⁰V. Moldoveanu and B. Tanatar, *Phys. Rev. B* **81**, 035326 (2010).
- ⁵¹C. Herrmann, G. C. Solomon, and M. A. Ratner, *J. Chem. Phys.* **134**, 224306 (2011).
- ⁵²S. Loth, K. von Bergmann, M. Ternes, A. F. Otte, C. P. Lutz, and A. J. Heinrich, *Nat. Phys.* **6**, 340 (2010).
- ⁵³T. Komeda, H. Isshiki, J. Liu, Y.-F. Zhang, N. Lorente, K. Katoh, B. K. Breedlove, and M. Yamashita, *Nat. Commun.* **2**, 217 (2011).
- ⁵⁴N. Lorente, R. Rurali, and H. Tang, *J. Phys.: Condens. Matter* **17**, S1049 (2005).
- ⁵⁵N. Bode, L. Arrachea, G. S. Lozano, T. S. Nunner, and F. von Oppen, *Phys. Rev. B* **85**, 115440 (2012).
- ⁵⁶A. J. Heinrich, J. A. Gupta, C. P. Lutz, and D. M. Eigler, *Science* **306**, 466 (2004).
- ⁵⁷C. F. Hirjibehedin, C. P. Lutz, and A. J. Heinrich, *Science* **312**, 1021 (2006).
- ⁵⁸C. F. Hirjibehedin, C.-Y. Lin, A. F. Otte, M. Ternes, C. P. Lutz, B. A. Jones, and A. J. Heinrich, *Science* **317**, 1199 (2007).
- ⁵⁹X. Chen, Y.-S. Fu, S.-H. Ji, T. Zhang, P. Cheng, X.-C. Ma, X.-L. Zou, W.-H. Duan, J.-F. Jia, and Q.-K. Xue, *Phys. Rev. Lett.* **101**, 197208 (2008).
- ⁶⁰J. Fernández-Rossier, *Phys. Rev. Lett.* **102**, 256802 (2009).
- ⁶¹F. Delgado, J. J. Palacios, and J. Fernández-Rossier, *Phys. Rev. Lett.* **104**, 026601 (2010).
- ⁶²F. Delgado and J. Fernández-Rossier, *Phys. Rev. B* **82**, 134414 (2010).
- ⁶³M. Persson, *Phys. Rev. Lett.* **103**, 050801 (2009).
- ⁶⁴J. Fransson, *Nano Lett.* **9**, 2414 (2009).
- ⁶⁵J. Fransson, O. Eriksson, and A. V. Balatsky, *Phys. Rev. B* **81**, 115454 (2010).
- ⁶⁶N. Lorente and J.-P. Gauyacq, *Phys. Rev. Lett.* **103**, 176601 (2009).
- ⁶⁷A. Hurley, N. Baadji, and S. Sanvito, *Phys. Rev. B* **84**, 035427 (2011).
- ⁶⁸T. Kurikawa, M. Hirano, H. Takeda, K. Yagi, K. Hoshino, A. Nakajima, and K. Kaya, *J. Phys. Chem.* **99**, 16248 (1995).
- ⁶⁹D. Rayane, A.-R. Allouche, R. Antoine, M. Broyer, I. Compagnon, and P. Dugourd, *Chem. Phys. Lett.* **375**, 506 (2003).
- ⁷⁰H. Xiang, J. Yang, J. G. Hou, and Q. Zhu, *J. Am. Chem. Soc.* **128**, 2310 (2006).
- ⁷¹K. Tao, V. S. Stepanyuk, P. Bruno, D. I. Bazhanov, V. V. Maslyuk, M. Brandbyge, and I. Mertig, *Phys. Rev. B* **78**, 014426 (2008).
- ⁷²R. Xiao, D. Fritsch, M. D. Kuzmin, K. Koepf, H. Eschrig, M. Richter, K. Vietze, and G. Seifert, *Phys. Rev. Lett.* **103**, 187201 (2009).
- ⁷³S. Sen and S. Chakrabarti, *J. Am. Chem. Soc.* **132**, 15334 (2010).
- ⁷⁴M. Karolak, D. Jacob, and A. I. Lichtenstein, *Phys. Rev. Lett.* **107**, 146604 (2011).
- ⁷⁵D. Rai, O. Hod, and A. Nitzan, *J. Phys. Chem. C* **114**, 20583 (2010).
- ⁷⁶G. Baym, *Phys. Rev.* **127**, 1391 (1962).
- ⁷⁷T.-H. Park and M. Galperin, *Phys. Rev. B* **84**, 205450 (2011).
- ⁷⁸Y. A. Izyumov, *AIP Conf. Proc.* **678**, 181 (2003).
- ⁷⁹A. V. Balatsky, Y. Manassen, and R. Salem, *Phys. Rev. B* **66**, 195416 (2002).
- ⁸⁰R. Pariser and R. G. Parr, *J. Chem. Phys.* **21**, 466 (1953); **21**, 767 (1953).
- ⁸¹J. A. Pople, *Trans. Faraday Soc.* **49**, 1375 (1953).
- ⁸²J.-X. Zhu and A. V. Balatsky, *Phys. Rev. Lett.* **89**, 286802 (2002).
- ⁸³Z. G. Yu, *J. Phys.: Condens. Matter* **22**, 295305 (2010).
- ⁸⁴A. Fuhrer, T. Ihn, K. Ensslin, W. Wegscheider, and M. Bichler, *Phys. Rev. Lett.* **93**, 176803 (2004).
- ⁸⁵G. D. Mahan, *Many-Particle Physics* (Plenum, New York, 1990).
- ⁸⁶H. Haug and A.-P. Jauho, *Quantum Kinetics in Transport and Optics of Semiconductors* (Springer, Berlin, 1996).
- ⁸⁷D. M. Newns, *Phys. Rev.* **178**, 1123 (1969).
- ⁸⁸A.-P. Jauho, N. S. Wingreen, and Y. Meir, *Phys. Rev. B* **50**, 5528 (1994).
- ⁸⁹E. U. Condon and G. H. Shortley, *The Theory of Atomic Spectra* (Cambridge University Press, Cambridge, 1964).
- ⁹⁰J. D. Jackson, *Classical Electrodynamics* (Wiley, New York, 1998).
- ⁹¹M. Büttiker, Y. Imry, and M. Ya. Azbel, *Phys. Rev. A* **30**, 1982 (1984).
- ⁹²M. Galperin, M. A. Ratner, and A. Nitzan, *J. Chem. Phys.* **121**, 11965 (2004).
- ⁹³W. Wang, T. Lee, I. Kretzschmar, and M. A. Reed, *Nano Lett.* **4**, 643 (2004).
- ⁹⁴Q.-f. Sun, X. C. Xie, and J. Wang, *Phys. Rev. B* **77**, 035327 (2008).
- ⁹⁵G. C. Solomon, D. Q. Andrews, R. P. Van Duyne, and M. A. Ratner, *ChemPhysChem* **10**, 257 (2009).
- ⁹⁶S. Yeganeh, M. A. Ratner, M. Galperin, and A. Nitzan, *Nano Lett.* **9**, 1770 (2009).
- ⁹⁷X. Xiao, B. Xu, and N. J. Tao, *Nano Lett.* **4**, 267 (2004).
- ⁹⁸Z. Xie, T. Z. Markus, S. R. Cohen, Z. Vager, R. Gutierrez, and R. Naaman, *Nano Lett.* **11**, 4652 (2011).
- ⁹⁹In realistic situation of a molecular junction one can not guarantee that the external field will be exactly normal to the molecular plane. In this case projection of the external field on the direction perpendicular to the plane is relevant for the model considered. An in-plane magnetic field causes only diamagnetic shift of electronic states. Such fields (together with electric gate potentials) are used in experiments for tuning (see e.g. Ref. 84), and are of secondary importance in our study.
- ¹⁰⁰The Green function is block diagonal in spin space due to effective second order in spin-spin coupling considered in the present work. Spin non-diagonal matrix elements appear in higher order considerations which for relatively weak spin-spin exchange coupling may be neglected. We note, that the result is similar to that obtained previously.⁶⁷
- ¹⁰¹Note that the explicit position of the LUMO in our model calculation is of secondary importance. Indeed, the IETS signal is demonstrated for gated junction (see Figs. 2 and 3), while for behavior at resonance LUMO only defines threshold bias.
- ¹⁰²Note that for the models considered, Eqs. (6), at most nearest neighbor contribution to the sum exists.